JOURNAL OF SOLID STATE CHEMISTRY 50, 362–371 (1983)

Comparison of the Force Field in Various Pyrochlore Families. I. The $A_2B_2O_7$ Oxides

M. T. VANDENBORRE* AND E. HUSSON

*Centre de Recherche, Ecole Centrale des Arts et Manufactures, 92290 Chatenay Malabry, and *Laboratoire de Spectrochimie du Solide, Université P. et M. Curie, 4 place Jussieu, 75230 Paris Cedex 05, France*

Received June 6, 1983; in revised form August 8, 1983

A complete vibrational study of various pyrochlore compounds $A_2B_2O_7$ shows the role of the different chemical bonds in the structure and how the physico-chemical characteristics of the A and B cations influence these bonds and the rigidity of the two lattices of the structure. Relations between vibrational spectra and structural features are established.

Introduction

A normal coordinate analysis has been undertaken on several families of pyrochlore compounds (*1–3*). We have considered first oxides of formula $A_2B_2O_7$, then other phases exhibiting structural defects such as nonstoichiometry, vacancies, substitutions, distortions, shear planes, etc. This work deals with the influence of the structural framework on the force constants of the chemical bonds and with the relationship between the calculated force field and the physico-chemical characteristics of the cations. Some results concerning the $A_2B_2O_7$ families are compared.

Experimental Results

The compounds have been synthesized by heating in air of a mixture of the oxides BO_2 or B_2O_5 and AO or A_2O_3 (pure at 99.9%), placed in an electric furnace CIF SM5. Stoichiometric quantities, of the mixture are finely ground, then pressed into disks at a pressure of 200 kg/cm^2. The disks are put into platinum crucibles, which are placed in an alumina cage. Well-crystallized compounds were obtained by heating at a temperature of 1400°C for 4 hr (titanates), 1500°C for 1 hr (stannates), 1200°C for 10 hr ($Cd_2Nb_2O_7$, $Cd_2Ta_2O_7$), and 650°C for 5 days ($Cd_2Sb_2O_7$). The spectra of zirconates and hafnates are described by Gundovin *et al.* (*4*).

The infrared spectra were recorded with a Perkin–Elmer 580 spectrometer between 4000 and 180 cm^{-1}. For the lower frequencies, a Perkin–Elmer 180 spectrophotometer or a NPL-Grubb Parson Fourier transform interferometer was used. The samples were in form of powder dispersed in cesium iodide discs or in polyethylene films.

The Raman spectra were recorded with Raman spectrometers Coderg PH1 and T800 using krypton radiation at 647.1 nm and argon radiation at 514.5 nm, with a power of about 400 mW and a slit width varying between 1 and 2 cm^{-1}.

0022-4596/83 $3.00

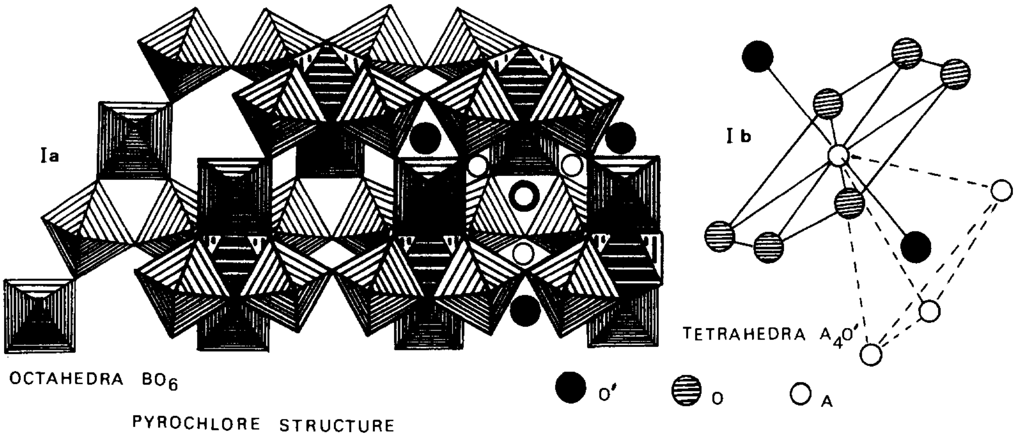

FIG. 1. Association of the octahedra and tetrahedra in the pyrochlore structure.

Comparison of the Spectroscopic Results

The following oxides have been compared:

titanates $Ln_2Ti_2O_7$ (Ln = Sm, Gd, Yb; Y) (*1*),
zirconates $La_2Zr_2O_7$ and $Nd_2Zr_2O_7$ (*2*),
hafnates $La_2Hf_2O_7$ and $Nd_2Hf_2O_7$ (*2*),
stannates $Ln_2Sn_2O_7$ (Ln = La, Sm, Gd, Yb, Lu; Y) (*1*),
a niobate $Cd_2Nb_2O_7$ (*3*),
a tantalate $Cd_2Ta_2O_7$ (*3*),
an antimonate $Cd_2Sb_2O_7$ (*3*).

All these compounds exhibit the pyrochlore structure, with space group $Fd3m$ (O_h^7) and eight formula units $A_2B_2O_6O'$ per unit cell. The structure is made of a network of BO_6 octahedra sharing all their corners around hexagonal vacancies, and a lattice of A_4O' tetrahedra positioned inside the vacancies (Fig. 1a). All the B–O bonds are equivalent (about 0.20 nm) and each A atom is bonded to two kinds of oxygen atoms: six oxygen atoms O belonging to the BO_6 octahedra (A–O bonds of about 0.26 nm) and two independent oxygen atoms O′ (A–O′ bonds of about 0.23 nm) (Fig. 1b).

Bhagavantam's method (*5*) gives the following representation for the vibrations of the pyrochlore structure $A_2B_2O_6O'$:

$$\begin{array}{llllllll} \Gamma_{\text{opt}} = & A_{1g} & + & E_g & + & 2F_{1g} & + & 4F_{2g} \\ & \text{(R)} & & \text{(R)} & & \text{(i)} & & \text{(R)} \\ + & 3A_{2u} & + & 3E_u & + & 7F_{1u} & + & F_{2u} \\ & \text{(i)} & & \text{(i)} & & \text{(ir)} & & \text{(i)} \end{array} \qquad \Gamma_{\text{ac}} = F_{1u}$$

(R = Raman active, ir = infrared active, i = inactive). Thus, six Raman lines (A_{1g}, E_g, and F_{2g}) and seven infrared bands (F_{1u}) are expected.

The comparison of the results for the different families yielded information on some general characteristics of the ir and Raman spectra and force field constants relative to the pyrochlore structure.

Figures 2 and 3 show the spectra of six oxides. The frequencies are reported on Table I. Most of the infrared spectra exhibit seven well-resolved absorption bands. The highest frequency band is usually broadened with an occasional shoulder as for $Cd_2Ta_2O_7$; this may be due to distortions in the BO_6 octahedra: the B–O bonds which should actually exhibit the same length and rigidity seem in such cases to be different. Raman spectra are more difficult to analyze. Only three lines have a strong intensity; additional lines sometimes appear on the low frequency range that cannot be accounted for in our calculations.

The normal coordinate analysis was pre-

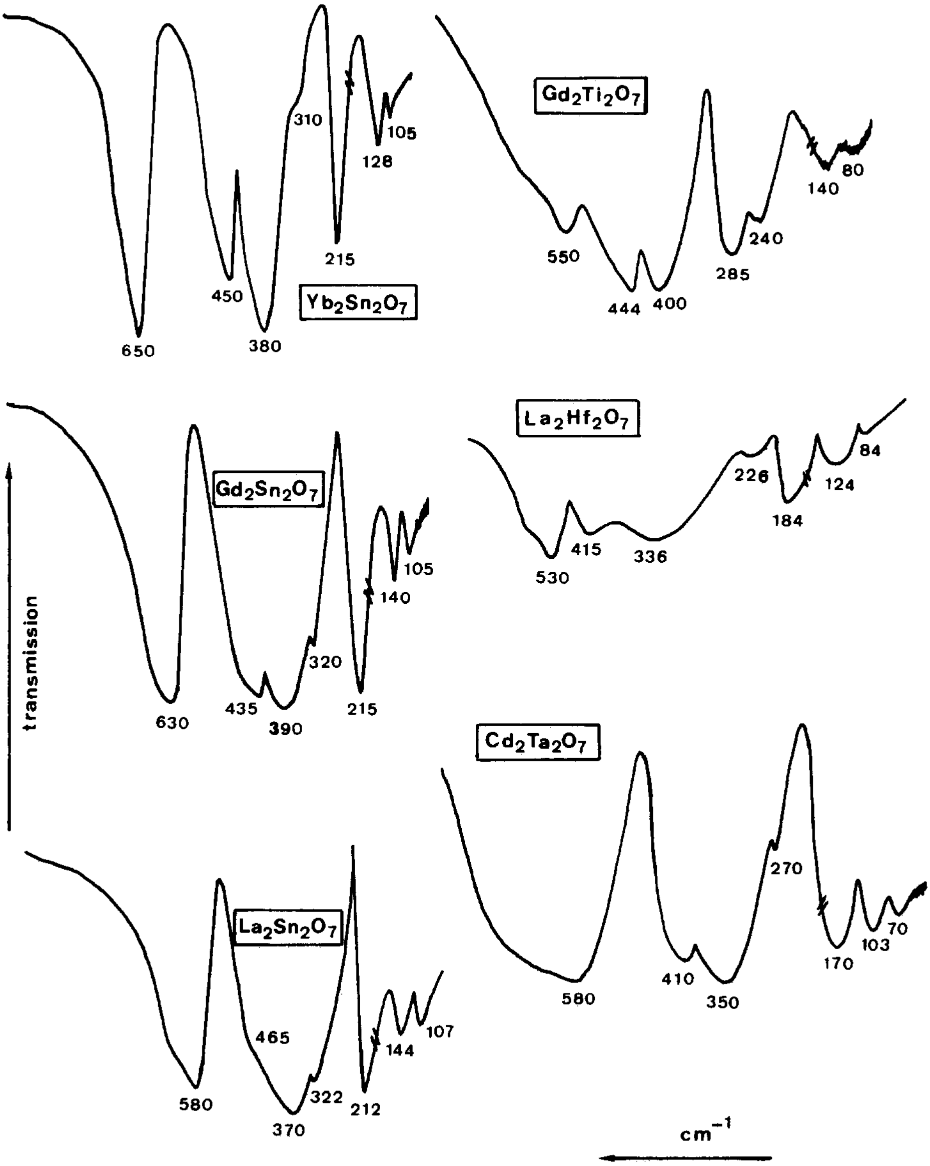

FIG. 2. Examples of absorption ir spectra for pyrochlore compounds.

viously described (*1*, *2*). We have used Wilson's method (*6*) and the Schachtschneider programs (*7*). Following Shimanouchi's method, we have considered a tridimensional infinite crystal, and used the Born von Kármán approximation (two neighboring cells vibrate in phase and $\mathbf{q}$ = O on the dispersion curves). We have chosen a generalized valence force field with the diagonal and interaction constants as defined in Table II. A few diagonal constants had very small values; these were set equal to zero; the same was done with several interaction constants of the types *fdd*,

TABLE I

COMPARISON OF THE ir AND RAMAN FREQUENCIES OF THE DIFFERENT COMPOUNDS (OBSERVED FREQUENCIES OF ZIRCONATES AND HAFNATES BELONGING TO 4), $r = \Sigma(f_{\text{obs}} - f_{\text{calc}})/\Sigma f_{\text{obs}}\%$.

	$Sm_2Ti_2O_7$	$Gd_2Ti_2O_7$	$Y_2Ti_2O_7$	$Yb_2Ti_2O_7$	$La_2Zr_2O_7$	$Nd_2Zr_2O_7$	$La_2Hf_2O_7$	$Nd_2Hf_2O_7$	$La_2Sn_2O_7$	$Sm_2Sn_2O_7$	$Gd_2Sn_2O_7$	$Y_2Sn_2O_7$	$Yb_2Sn_2O_7$	$Lu_2Sn_2O_7$	$Cd_2Ta_2O_7$	$Cd_2Nb_2O_7$	$Cd_2Sb_2O_7$	Mode
Infrared (cm^{-1})																		
	640	640	—	—	610	610	620	—	635	—	—	—	—	—	640	640	—	—
	550	550	568	570	518	527	532	550	580	617	630	640	650	652	580	580	760	F_{1u}
	440	444	462	450	412	421	415	412	465	430	435	454	450	458	410	430	465	F_{1u}
	400	400	410	400	352	372	336	358	370	385	390	396	380	390	350	375	360	F_{1u}
	240	240	248	235	244	226	226	222	322	320	320	350	310	310	270	280	290	F_{1u}
	285	285	285	270	208	187	184	176	212	215	215	227	215	215	170	215	230	F_{1u}
	140	140	176	136	140	132	124	134	144	142	140	176	128	126	103	107	117	F_{1u}
	78	80	105	75	101	70	84	68	107	105	105	125	102	100	70	74	78	F_{1u}
Raman (cm^{-1})																		
	700	705	717	720	743	733	762	759	—	—	—	—	—	—	720	650		—
	580	580	586	590	590	590	575	585	600	608	610	610	618	620	575	580		F_{2g}
	515	515	527	525	523	532	523	523	530	530	530	530	530	530	524	510		F_{2g}
	515	515	527	525	498	523	498	503	495	500	502	505	508	510	524	510		A_{1g}
	348^a	347^a	333	350^a	395	395	395	395	406	410	415	418	417	418	333	335		E_g
	317	317	318	320	298	305	295	306	340	344	346	355	360	360	298	285		F_{2g}
	225	227	227	220	240^a	216^a	225^a	215^a	304	308	310	315	312	312	245	260^a		F_{2g}
	215	215	218	205	—	—	—	—	—	—	—	—	—	—	180	153		—
	110	110	114	—	—	—	—	—	—	—	—	—	—	—	142	95		—
r(%)	2.0	1.9	2.1	1.9	1.9	2.7	2.4	2.5	1.9	1.7	1.6	1.7	1.5	1.6	1.4	1.6	1.3	

[a] Frequencies calculated and not observed.

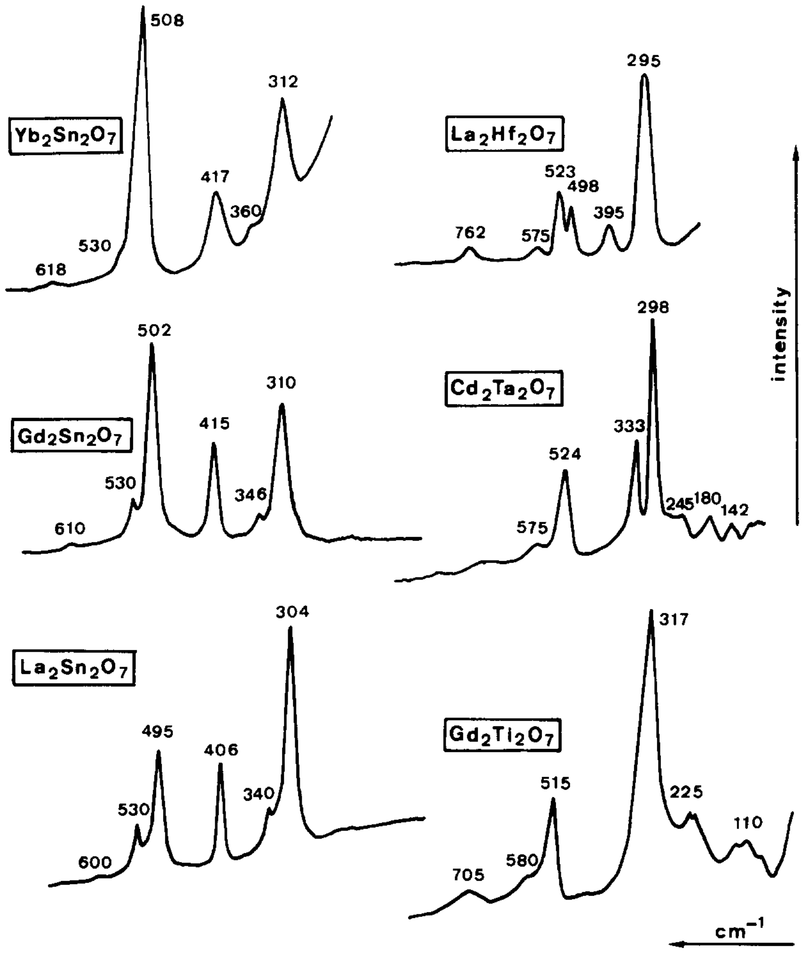

FIG. 3. Examples of Raman scattering spectra for pyrochlore compounds.

fda, and *faa*, which had no noticeable influence on the force field, in order that the number of constants was reduced below the number of observed frequencies. Ten force and interaction constants were necessary to define our force field for the pyrochlore compounds. All the force constants are calculated for each compound; however in Table II, we provide the average value of the constants which are similar for all the compounds. The principal and interesting force constants are reported in Table III for each compound. The average error $r = \Sigma(f_{\text{observed}} - f_{\text{calculated}})/\Sigma f_{\text{observed}}$ transcribed in Table I, is always less than 2.5%. The difference between the calculated and observed frequencies is less than 15 cm^{-1}.

TABLE II

GENERAL PYROCHLORE FORCE FIELD

Stretching B–O (d)	Between 1.00 and 2.50 N/cm
Interaction O_1–B_1/B_1–O_2 opposed (d^0)	0.10–0.30
Interaction O_1–B_1/B_1–O_3 at 90° (d^*)	<0.20
Bending O_1–B_1–O_2 (a)	~1.00
Bending O_1–B_1–O_3 (a')	~1.00
Interaction O_1–B_1–O_2/O_2–B_1–O_3 (aa)	<0.15
Stretching A–O (D)	0.20–0.30
Bending O–A–O (b)	~0.20
Stretching A–O′ (D')	0.20–0.50
Bending O–A–O′ (b')	~0.20

TABLE III

PRINCIPAL FORCE CONSTANTS OF DIFFERENT PYROCHLORE FAMILIES

	Force field (N/cm)				Lengths (nm)			Mass (g) (*18*)		Electronegativeness (*19*)	
	B–O	O–*B*–O	*A*–O	*A*–O′	*B*–O	*A*–O	*A*–O′	*A*	*B*	*A*	*B*
$Sm_2Ti_2O_7$	1.27	1.00	0.20	0.24	0.197	0.252	0.221	150.35	47.90	1.1	1.4
$Yb_2Ti_2O_7$	1.32	1.00	0.20	0.24	0.192	0.252	0.218	173.04	47.90	1.2	1.4
$La_2Zr_2O_7$	1.50	1.10	0.26	0.24	0.210	0.266	0.234	138.92	91.22	1.1	1.4
$La_2Hf_2O_7$	1.57	1.11	0.26	0.24	0.209	0.264	0.233	138.92	178.49	1.1	1.3
$La_2Sn_2O_7$	1.73	0.97	0.32	0.37	0.207	0.264	0.232	138.92	118.69	1.1	1.8
$Gd_2Sn_2O_7$	1.90	0.96	0.31	0.38	0.205	0.254	0.227	157.26	118.69	1.1	1.8
$Y_2Sn_2O_7$	1.96	0.97	0.34	0.44	0.205	0.249	0.225	88.92	118.69	1.2	1.8
$Lu_2Sn_2O_7$	2.04	0.95	0.29	0.37	0.204	0.245	0.223	174.79	118.69	1.2	1.8
$Cd_2Ta_2O_7$	1.53	1.08	0.12	0.30	0.196	0.265	0.225	112.41	180.95	1.7	1.5
$Cd_2Nb_2O_7$	1.45	1.00	0.11	0.35	0.196	0.265	0.225	112.41	92.91	1.7	1.6
$Cd_2Sb_2O_7$	2.5	0.80	0.14	0.35	0.194	0.262	0.222	112.41	121.75	1.7	1.9

Discussion

Force Field Characteristics

The *B*–O lattice always appears to be more rigid, with greater stretching and bending constants than the *A*–O lattice. This arises from the fact that *B*–O bonds link octahedra together and therefore are mainly responsible for the cohesion of the crystal. They exhibit a more covalent character than *A*–O or *A*–O′ bonds. No simple relationship between the stretching force constants and the length of the bonds exists. The constants may vary with the nature of the bonds (degree of covalency) and with their role in the structure and their chemical environment.

The bending constants f(O–*B*–O) are fairly large for all the pyrochlores (about 1 N · cm^{-1}) in comparison to the stretching constants f(*B*–O) (1.30 to 2.50 N · cm^{-1}). These constants depend on the spatial ordering of the octahedra rather than on the nature of cations *A* or *B*.

Compared with others structures or anions (*8–13*), the stretching constants *B*–O are similar to those for octahedra sharing corners. They are weaker than those for octahedra sharing edges. However, the bending constants f(O–*B*–O) are greater than in other structures. Because of the geometry of the large vacancies, the angular constraints are certainly much stronger in the pyrochlore structure.

Variation of the B–O Stretching Constants with the B Cation

The f(*B*–O) constants depend on the electronegativity of the B^{n+} cation, i.e., the covalency of the *B*–O bond. Therefore, the greatest force constants are found in stannates and antimonates. Moreover, the stronger the field induced by the B^{n+} cation among the octahedra network, the larger is the force field of the whole crystal. This phenomenon has also been pointed out by Saine (*12*) in the case of rare earth gallates and aluminates. Strongly covalent bonds such as Sn–O bonds are influenced by slight variations of the crystal cell. This does not happen with ionic and less rigid bonds.

In the case of transition elements with

very similar electronegativities, the force field depends on the atomic number. The force constants ratio of two elements situated in the same column of the periodic table has a nearly constant value:

$$\frac{f(\mathrm{Nb–O})}{f(\mathrm{Ta–O})} \simeq \frac{f(\mathrm{Ti–O})}{f(\mathrm{Zr–O})} \simeq \frac{f(\mathrm{Zr–O})}{f(\mathrm{Hf–O})} \simeq 0.8 \text{ at } 0.9.$$

This phenomenon masks the mass effect; hence, the vibrational spectra of the niobates and tantalates, for example, are very similar, despite the difference in mass of the Nb^{5+} and Ta^{5+} cations.

Comparison of the Stretching Constants of the A–O Bonds

According to our calculations $f(A\text{–O})$ and $f(A\text{–O}')$ force constants are six to eight times weaker than those of $f(B\text{–O})$. Considering the bond length, we should expect higher force constants for A–O′ bonds (0.23 nm) than for A–O bonds (0.26 nm). In the cadmium niobate, tantalate, and antimonate, the A–O′ bonds are three times stronger than the A–O bonds (about 0.35 and 0.12 N · cm^{-1}, respectively); but in the rare-earth series (zirconates, hafnates, titanates, stannates) the force constants $f(A\text{–O})$ and $f(A\text{–O}')$ are almost the same. It is well known that the rare-earth cations generally establish ionic bonds with oxygen and thus have weak force constants which are weakly influenced by the chemical environment; by contrast, the cadmium orbitals may exhibit a *sp* hybridization leading to a relative strengthening of the A–O′ bonds.

In rare-earth series, our results seem to contradict the structural data but are in agreement with the chemical features of these compounds: there are some $A_2B_2O_6$ oxides in which A–O′ bonds do not exist and this fact is consistent with a weak force constant for these bonds. We may conclude that there is a statistical delocalization of the A cations, which would place it closer to some O oxygen atoms. This would lead to an average position of the A cation as determined by X-ray diffraction, i.e., in this case, a minimal length for the A–O′ bonds.

Comparison with Calculations of Lattice Energy and Discussion Concerning the Structure

(1) Barker (*14*) and Pannetier (*15, 16*) have calculated the lattice energies and the Madelung constants for several pyrochlore oxides. As did these authors, we encountered a weaker interaction in the $A_2^{\mathrm{II}}B_2^{\mathrm{V}}O_7$ compounds than in the $A_2^{\mathrm{III}}B_2^{\mathrm{IV}}O_7$ series. However, the lattice energy calculations seem to show that the $A_2^{\mathrm{II}}B_2^{\mathrm{V}}O_7$oxides are more stable than the others. Now, our results show a difference of rigidity in the structures, mainly related to the electronegativity of the B cation, and therefore to the covalency of the B–O bond. This rigidity must be reexamined with each B cation. It is not really surprising that spectroscopic methods and lattice energy calculations lead to different results. These calculations take into account only the electrostatic forces (attraction, repulsion, and interaction) which are minimized in the force field calculation by the Wilson method; in this method, the chemical bonds selected are those which ensure the cohesion of the crystalline framework, i.e., the more covalent bonds. In fact, the rigidity (represented by the force constant) is related to the nature of the cations and anions and, therefore, to the chemical bond which is established; that may be very different from the bond energy or from the lattice energy which correspond to the energy necessary to break the bonds. This fact had already been noted for very simple compounds such as HCl or NaCl by Weigel (*20*).

(2) An analysis of the spectra profile yields more information concerning the local distortions of the structure or about order–disorder phenomena:

Rare-earth stannates appear to be very stable and exhibit a very regular structure. The pyrochlore structure exists for the whole rare-earth series and the vibrational spectra are very well resolved; only in $La_2Sn_2O_7$ does the highest infrared frequency band exhibit a shoulder, suggesting a slight distortion of the SnO_6 octahedra.

In the rare-earth zirconates, according to Sheetz and White (*21*) and Michel (*22*), an intrinsic disorder within the structure would exist, associated with the presence of pyrochlore and fluorite domains. This fact is responsible for the poor resolution or the broadness of the ir and Raman spectra.

For the rare-earth zirconates, Sheetz and White (*21*) postulate a structure involving a dynamically disordered array of dipoles exists caused by a slight shift of the titanium away from the center of the octahedron. This explains the broadness of the ir bands and the rather good quality of the Raman spectra of these compounds; for, in the Raman active modes the *A* and *B* cations which are theoretically located on the inversion center do not contribute to the vibrations; only vibrations of the oxygen atoms are possible. This is why the Raman modes are less affected by the disorder than the ir modes involving the vibrations of the cations.

For niobate and tantalate, we observe the same features as for titanates but the highest ir frequency band is very strong. This suggests a large distribution of the Nb–O or Ta–O bond lengths in the BO_6 octahedra. By contrast, the antimonate and stannate spectra are well resolved.

In conclusion, stannates and antimonates seem to exhibit a more regular pyrochlore structure than transition metal *B* cations. Indeed, transition metal cations such as Ti^{4+}, Zr^{4+}, Nb^{5+}, Ta^{5+} have the nd^0 electronic configuration and therefore exhibit a large polarizability (*21*) that can induce a distortion of the *B* cations position leading to a dynamic disorder. This disorder can explain the appearance of some additional lines on the Raman spectra specially for titanates, niobates, and tantalates. In these compounds, the structure determined by X-ray diffraction is statistically cubic. A similar phenomenon has already been noted in some perovskite oxides by X-ray diffusion

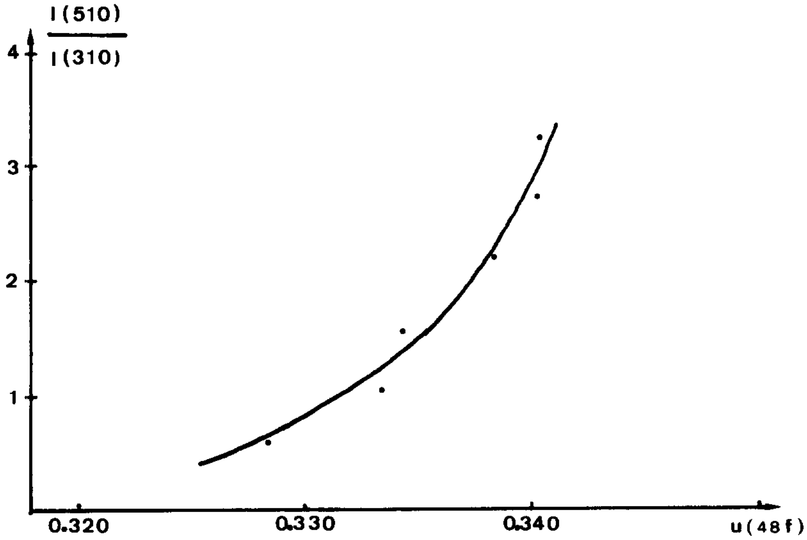

FIG. 4. Variation of ratio $r = I_{(510)}/I_{(310)}$ with the $u(48f)$ parameter.

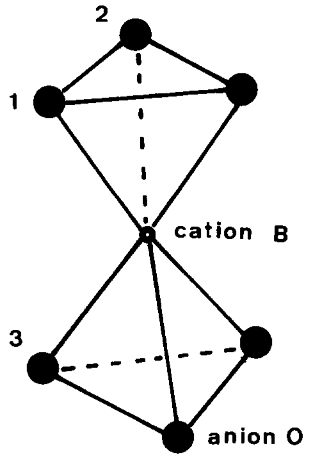

FIG. 5. Deformation of the BO_6 octahedra with $u(48f)$ according to 17.

methods (*24*) or infrared spectroscopy (*25*). By contrast, Sb^{5+} and Sn^{4+} cations having a nd^{10} electronic configuration, have a weaker polarizability, and would be more ordered.

(3) It is also possible to relate the profile of the spectra to the geometry of the structure. The Raman spectra of rare-earth stannates $Ln_2Sn_2O_7$ (Ln = La, Sm, Gd, Yb, Lu) exhibit a variation of the intensity of the A_{1g} line near 510 cm^{-1}, corresponding mainly to the SnO_6 octahedra vibrations (*1*), and of the F_{2g} line near 310 cm^{-1} arising from the vibration of the A–O and A–O′ lattice. The ratio $I_{(510)}/I_{(310)}$ was plotted versus the structural parameter $u(48f)$ of the oxygen position in the structure. A regular variation of the phenomenon along the rare-earth series is observed (Fig. 4).

It is well known and has been recently again been pointed out by McCauley (*17*) that in a pyrochlore compound, the BO_6 octahedra are stretched or squashed along the $\bar{3}$ axis if the $u(48f)$ parameter (origin on B; $\bar{3}$ m) differs from 0.3125. When the BO_6 polyhedron is more regular, the AO_8 polyhedron becomes more distorded and vice versa. We propose that in the series $La_2Sn_2O_7$ to $Lu_2Sn_2O_7$ the relative directions of the Sn–O (and Ln–O) bonds vary slightly as do the repulsion forces between the oxygen atoms of a same basal plane (O_1 and O_2; Fig. 5) and the oxygen atoms of two opposite planes (O_1 and O_3; Fig. 5). This would induce a variation in the polarizability of Sn–O (and Ln–O) bonds, leading to a more intense Raman line when the polyhedron is more distorded. Thus, the Raman spectra SnO_6 or LnO_8 would be strongly influenced by even a very slight variation in the structure geometry.

Conclusion

This study of the different $A_2B_2O_7$ pyrochlore families provided information on the vibrational spectra and force field of such compounds. Interesting results about the pyrochlore structures have also been obtained. The vibrational spectra yield information on the bond rigidity, together with the local order or disorder and the local geometry of the polyhedra. Thus, it becomes possible, from the vibrational spectra alone, to determine whether a compound exhibits a pyrochlore structure and also to forecast some of its structural characteristics. An analysis of the vibrational spectra of pyrochlore phases presenting structural defects will be presented in a forthcoming paper.

References

1. M. T. VANDENBORRE, E. HUSSON, J. P. CHATRY, AND D. MICHEL, *J. Raman Spectrosc.* **14**(2), 63 (1983).
2. M. T. VANDENBORRE, E. HUSSON, AND H. BRUSSET, *Spectrochim. Acta Part A* **37**, 113 (1981).
3. M. T. VANDENBORRE, E. HUSSON, AND J. L. FOURQUET, *Spectrochim. Acta Part A* **38**(9), 997 (1982).
4. N. V. GUNDOVIN, F. M. SPIRIDONOV, L. N. KOMISSAROVA, AND K. I. PETROV, *Zh. Neorg. Khim.* **20**, 582 (1975).
5. S. BHAGAVANTAM AND T. VENKATARYUDU, *Proc. Indian Acad. Sci.* **19**, 224 (1939).

6. E. B. Wilson, J. C. Decius, and P. C. Cross, "Molecular Vibrations, The Theory of Infrared and Raman Vibrational Spectra." McGraw–Hill, New York (1955).
7. J. H. Schachtschneider, Shell Development Co. Tech. Rep. 231-264, Vol. 57-65 (1964).
8. Parvez Ahmad and Nitish K. Sanyal, *Spectrosc. Lett.* **9**(1), 39 (1976).
9. E. Husson, Y. Repelin, N. Q. Dao, and H. Brusset, *Mater. Res. Bull.* **12,** 1199 (1977).
10. Y. Repelin, E. Husson, and H. Brusset, *Spectrochim. Acta Part A* **35,** 937 (1979).
11. M. T. Vandenborre, Thèse Doc.es Sciences, Paris, 1981.
12. M. C. Saine, E. Husson, and H. Brusset, *Spectrochim. Acta Part A* **38**(1), 19 (1982).
13. M. T. Vandenborre, E. Husson, and H. Brusset, *Spectrochim. Acta Part A* **37,** 113 (1981).
14. W. W. Barker, J. Graham, O. Knop, and F. Brisse, Chem. Extented Defects Nonmetals Solids, Proceedings, Institute Advanced Study, p. 198–206, North-Holland, Amsterdam (1979).
15. J. Pannetier, Thèse Doc.es Sciences, Rennes, 1974.
16. Y. Calage and J. Pannetier, *J. Phys. Chem. Solids* **38,** 711 (1977).
17. R. A. McCauley, *J. Appl. Phys.* **51**(1), 290 (1980).
18. Tables des masses atomiques relatives, *Bull. Soc. Chim. Fr.* (1962). $C = 12.000000$.
19. L. Pauling, "The Chemical Bond," Cornell Univ. Press, Ithaca, N.Y. (1967).
20. D. Weigel, *Rev. Phys. Appl.* **12**(5), 637 (1977).
21. Sheetz and White, Proceedings, Rare Earth Conference, Vol II, p. 524, 1976.
22. D. Michel, M. Perez, Y. Jorba, and R. Collongues, *Mater. Res. Bull.* **9,** 1457 (1974).
23. R. Comes, M. Lambert, and A. Guinier, *Acta Crystallogr. Sect. A* **26,** 244 (1970).
24. R. Comes, F. Denoyer, and M. Lambert, *J. Phys. Colloq. Orsay Fr.* C5a, 195 (1971).
25. E. W. Kaleveld, D. J. Bruntinck, J. P. Dotman, and G. Blasse, *J. Inorg. Nucl. Chem.* **35,** 3928 (1973).